

# Is There an Instability Transition in Standing Wave Traps?

BOGDAN MIELNIK

*Departamento de Física del CINVESTAV, México and Institute of Theoretical Physics of Warsaw University, Warsaw, Poland*

and

DAVID J. FERNÁNDEZ C.

*Departamento de Física del CINVESTAV, México*

(Received: 23 March 1988; revised version: 27 July 1988)

**Abstract.** For a class of standing electromagnetic waves of a special structure, the motion of the charged particles in the vicinities of nodal points is approximable by an exactly soluble dynamical model (the Schrödinger particle driven by a rotating magnetic field). This model shows a sudden qualitative change when the field intensity/frequency ratio crosses a critical value. It implies the conversion of the nodal points from particle traps into repulsive centers. A hypothesis is thus raised that for high intensity/frequency values, the standing wave traps can undergo a qualitative metamorphosis resembling the phase transitions.

AMS subject classifications (1980). Principal 70J30; secondary 81D99.

## 1. Introduction

The behavior of charged particles in quickly oscillating electromagnetic fields is a subject of increasing interest. It is motivated by the discovery of the ‘standing wave traps’ which permits the catching of charged (and/or neutral polarized) particles in crossed laser beams [1, 2]. The almost unique mathematical tool to predict the motion of classical or quantum objects in quickly oscillating fields is the ‘high frequency approximation’ [3–6]. It consists of neglecting the magnetic component and representing an average effect of the field oscillations by an ‘effective potential’ build-up out of the oscillating electric force. When this is monochromatic, e.g.  $\bar{E}(\bar{x}, t) = \bar{E}(\bar{x}) \sin \omega t$ , the effective potential becomes

$$\begin{aligned} V_{\text{ef}}(\bar{x}) &= \frac{1}{2m} \left( \frac{e}{\omega} \right)^2 \langle [\bar{E}(\bar{x}, t)]^2 \rangle_{\text{time average}}, \\ &= \frac{1}{4m} \left( \frac{e}{\omega} \right)^2 [\bar{E}(\bar{x})]^2 \end{aligned} \quad (1.1)$$

thus creating a ‘radiative analogue’ of a solid-state potential ( $V_{\text{ef}}$  periodic for uncomplicated standing waves), with attraction centers placed at the null points of the oscillating

electric force. By sticking consistently to this model, one might expect that by applying standing waves of the same frequency but growing intensity, one can only ‘improve the trap’ by increasing the attraction force of the nodal points. However, it turns out that once the particle is very near to one of the attraction centers, the high frequency approximation can be substituted by a more exact method which leads to different results.

## 2. The Nodal Point Approximation

We shall apply the alternative method to the standing waves of a special structure, where it works with exceptional simplicity (though it seems that a similar approach is more widely applicable). Consider the electromagnetic standing wave described by the four-vector potential  $(A^\circ, \bar{A})$ , where  $A^\circ \equiv 0$  and

$$\bar{A} = \bar{A}_{\bar{n}, \bar{s}}(\bar{x}, \omega t) = A\bar{n} \sin \frac{\omega\bar{s}\bar{x}}{c} \sin \omega t, \quad (2.1)$$

with  $\bar{n}, \bar{s}$  being two orthogonal unit vectors and  $A \in \mathbb{R}$  the wave amplitude. Let  $\bar{A}_{[\bar{n}, \bar{s}]}$  mean the ‘antisymmetric’ combination of two orthogonal standing waves

$$\bar{A}_{[\bar{n}, \bar{s}]} = \frac{1}{2}(\bar{A}_{\bar{n}, \bar{s}} - \bar{A}_{\bar{s}, \bar{n}}). \quad (2.2)$$

For  $\bar{n}, \bar{m}, \bar{s}$  denoting three mutually orthogonal unit vectors, consider now the following solution of the free Maxwell equations

$$A^\circ \equiv 0,$$

$$\begin{aligned} \bar{A}(\bar{x}, t) &= \bar{A}_{[\bar{n}, \bar{s}]}(\bar{x}, \omega t) + \bar{A}_{[\bar{m}, \bar{s}]}(\bar{x}, \omega t + \frac{\pi}{2}) \\ &= \frac{1}{2}A \left[ \left( \bar{m} \sin \frac{\omega\bar{s}\bar{x}}{c} - \bar{s} \sin \frac{\omega\bar{m}\bar{x}}{c} \right) \cos \omega t + \right. \\ &\quad \left. + \left( \bar{s} \sin \frac{\omega\bar{n}\bar{x}}{c} - \bar{n} \sin \frac{\omega\bar{s}\bar{x}}{c} \right) \sin \omega t \right]. \end{aligned} \quad (2.3)$$

The field (2.3) is a standing wave satisfying both Coulomb and Lorentz gauges and obtained by crossing four standing plane waves of type (2.1). As can be easily seen, it possesses a lattice of the nodal points, determined by the wavelength  $\lambda = 2\pi c/\omega$

$$\mathcal{N} = \{ \lambda(l_1\bar{n} + l_2\bar{m} + l_3\bar{s}) : l_1, l_2, l_3 = 0, \pm 1, \pm 2 \dots \} \star \quad (2.4)$$

where the local behavior of the electromagnetic forces becomes specially simple. Each point of  $\mathcal{N}$  is physically equivalent to the nodal point at  $\bar{x} = 0$ . In a close vicinity of this

★ The set  $\mathcal{N}$  does not exhaust all the nodal points of the field (2.3). Others can be obtained by taking  $l_1, l_2, l_3$  to be half-integers (see also Remark 2 of Section 4).

last one (i.e., for  $|\bar{x}| \ll \lambda/2$ ), the electromagnetic field (2.3) can be approximated by

$$\begin{aligned}\bar{A}(\bar{x}, t) &\cong -\frac{1}{2} \frac{A\omega}{c} \{[\bar{m}(\bar{s}\bar{x}) - \bar{s}(\bar{m}\bar{x})] \cos \omega t + [\bar{s}(\bar{n}\bar{x}) - \bar{n}(\bar{s}\bar{x})] \sin \omega t\} \\ &\cong -\frac{1}{2} \bar{x} \times \bar{B}(t),\end{aligned}\quad (2.5)$$

where

$$\begin{aligned}\bar{B}(t) &= B(\bar{n} \cos \omega t + \bar{m} \sin \omega t) \\ &= B\bar{n}(t); \quad \left(B = \frac{A\omega}{c}\right).\end{aligned}\quad (2.6)$$

The vector potential (2.5)–(2.6) can arise in quite independent physical circumstances, if one wants to describe the field of a rotating magnet in a ‘nonrelativistic approximation’ in which the retardation effects are neglected and the field is supposed to adjust itself instantaneously to the motion of the source. (Such a retardation-free picture is, in fact, adopted in the description of the magnetic pulses intervening in the spinecho effects [7, 8] as well as in the description of nonrelativistic particles in the time-dependent magnetic fields [9–10].) Within this doctrine, (2.5) is simply the vector potential of the homogeneous rotating magnetic field (2.6). Taking the approximate expression (2.5) as *bona fide*, we shall now show that the motion of the charged Schrödinger particle (as well as of a classical charged point particle) in the rotating field (2.5) is an exactly soluble dynamical process. Moreover, it turns out that for some values of the physical parameters, the resulting motion, even in the closest neighborhood of the nodal point, differs radically from the one predicted by (1.1).

### 3. The Motion of the Schrödinger Particle Driven by the Rotating Potential (2.5)

The motion of the Schrödinger particle in the field (2.5) is traditionally described by the time-dependent Hamiltonian

$$H(t) = \frac{1}{2m} \left( \bar{p} - \frac{e}{c} \bar{A}(\bar{x}, t) \right)^2 \quad (3.1)$$

leading to

$$\begin{aligned}H(t) &= \frac{1}{2m} \left( \bar{p} + \frac{1}{2} \bar{x} \times \bar{B}(t) \right)^2 \\ &= \frac{1}{2m} [\bar{p} + a^2 \bar{x}_\perp(t)]^2 - \frac{a}{m} \bar{n}(t) \bar{M},\end{aligned}\quad (3.2)$$

where

$$a = \frac{1}{2} \frac{eB}{c} = \frac{1}{2} \frac{eA\omega}{c^2},$$

$\bar{M}$  is the angular momentum operator,  $\bar{M} = \bar{x} \times \bar{p}$ ,  $\bar{n}(t)$  is the unit vector indicating the direction of  $\bar{B}(t)$ ,

$$\bar{n}(t) = \bar{n} \cos \omega t + \bar{m} \sin \omega t,$$

and  $\bar{x}_\perp(t)$  is the projection of the coordinate three-vector onto the direction orthogonal to  $\bar{n}(t)$

$$\bar{x}_\perp(t) = \bar{x} - (\bar{n}(t)\bar{x})\bar{n}(t). \quad (3.3)$$

Due to the particular time-dependence of  $\bar{n}(t)$  (which just rotates around the  $\bar{s}$ -axis), the Hamiltonian (4.1)–(4.2) can be expressed as

$$H(t) = e^{+it\omega\bar{M}\bar{s}} \frac{1}{m} \left[ \frac{\bar{p}^2}{2} + \frac{a^2}{2} \bar{x}_\perp^2 - a\bar{n}\bar{M} \right] e^{-it\omega\bar{M}\bar{s}}, \quad (3.4)$$

where  $\bar{x}_\perp = \bar{x}_\perp(0) = \bar{x} - (\bar{n}\bar{x})\bar{n}$ .

Henceforth, the differential equation for the evolution operator  $U(t)$ :

$$\frac{dU(t)}{dt} = -iH(t)U(t); \quad U(0) = 1, \quad (3.5)$$

can be simplified by the substitution

$$U(t) = e^{-it\omega\bar{M}\bar{s}} W(t), \quad (3.6)$$

interpreted as a transition to the rotating frame. The resulting differential equation for  $W(t)$  is

$$\frac{dW}{dt} = -iGW(t), \quad (3.7)$$

where  $G$  is the time-independent generator

$$G = \frac{1}{2m} \bar{p}^2 - \frac{a}{m} \bar{n}\bar{M} + \frac{1}{2m} a^2 \bar{x}_\perp^2 + \omega\bar{M}\bar{s}. \quad (3.8)$$

Taking the unit vectors  $\bar{n}$ ,  $\bar{m}$ ,  $\bar{s}$  in the directions of  $x$ ,  $y$ ,  $z$  axes respectively, this can be reduced, without losing generality, to

$$G = \frac{1}{2m} \bar{p}^2 + \frac{a^2}{2m} (y^2 + z^2) - \frac{a}{m} M_x + \omega M_z. \quad (3.9)$$

Since  $G$  is time-independent, Equation (3.7) is formally solved by  $W(t) = e^{-itG}$ , and since  $G$  is quadratic in  $\bar{x}, \bar{p}$ , it can also be explicitly solved [9, 12]. One of the easiest solutions [conserving a natural correspondence with the classical theory] consists of looking for the time-dependent images of the six canonical operators

$$q = \left\| \begin{array}{c} q_1 \\ \vdots \\ q_6 \end{array} \right\| = \left\| \begin{array}{c} \bar{x} \\ \bar{p} \end{array} \right\| \quad (3.10)$$

in the Heisenberg frame (the 'Heisenberg trajectory'). The differential equation for the time-dependent variables

$$\begin{aligned} q_j(t) &= W(t)^* q_j W(t) = e^{itG} q_j e^{-itG}; \\ \frac{dq_j(t)}{dt} &= [iG, q_j], \end{aligned} \quad (3.11)$$

reduces to the  $c$ -number matrix equation for the six component vector  $q(t)$

$$\frac{dq(t)}{dt} = \Lambda q(t), \quad (3.12)$$

where

$$\Lambda = \left\| \begin{array}{ccc|ccc} 0 & -\omega & 0 & 1/m & & \\ \omega & 0 & a/m & & 1/m & \\ 0 & -a/m & 0 & & & 1/m \\ \hline 0 & & & 0 & -\omega & 0 \\ & -a^2/m & & \omega & 0 & a/m \\ & & -a^2/m & 0 & -a/m & 0 \end{array} \right\|. \quad (3.13)$$

The solution of (3.12) is

$$q(t) = e^{t\Lambda} q, \quad (3.14)$$

and the corresponding canonical trajectory in the original, nonrotating frame can be obtained by adding to (3.14) a permanent rotational drift around the  $\bar{s}$  axis with the constant angular velocity  $\omega$ .<sup>★</sup> It now turns out that the solution (3.13)–(3.14) exhibits some properties which could not be anticipated on the basis of the 'high frequency approximation' (1.1).

<sup>★</sup> A complete study of the Heisenberg trajectory as well as of the behavior of the Schrödinger wave packets for the dynamical problem (3.1)–(3.2) is carried out elsewhere [12].

#### 4. Instability Threshold

The global character of the trajectories (3.14) depends on the algebraic type of the  $6 \times 6$  matrix (3.13), whose characteristic polynomial is

$$D_\Lambda(\lambda) = \text{Det}(\lambda - \Lambda) = \omega^6 \Delta(\sigma), \quad (4.1)$$

where  $\sigma := \lambda^2/\omega^2$  and

$$\Delta(\sigma) = \sigma^3 + 2(1 + 2\alpha^2)\sigma^2 + (1 + 3\alpha^2)\sigma + \alpha^2; \quad \left( \alpha = \frac{a}{m\omega} \right). \quad (4.2)$$

By virtue of Cardan's discriminant theory, the general properties of the matrix  $\Lambda$  (and, simultaneously, the character of the motion (3.14)) are defined by one dimensionless constant:

$$\alpha = \frac{a}{m\omega} = \frac{1}{2} \left( \frac{e}{m} \right) \frac{B}{\omega c} = \frac{1}{2} \frac{eA}{mc^2}. \quad (4.3)$$

Further on, the type of  $\Lambda$  changes when  $\alpha$  crosses the 'catastrophe value'

$$\alpha_c = 0.579982655598\dots \quad (4.4)$$

Below the critical value (4.4), the polynomial  $\Delta(\sigma)$  has three negative real roots  $\Rightarrow D_\Lambda(\lambda)$  has six purely imaginary eigenvalues and, therefore, the formula (3.14) defines 'circular motions' in the six-dimensional space of the canonical variables [12]. Within the range of values  $0 < \alpha < \alpha_c - v^2 \sec^2 \times 10^{-36}$  the resulting Heisenberg trajectory (as well as the drifting, time-dependent 'squeezed states' of the Schrödinger representation) show a good average agreement with the effective potential (1.1) [12]. However, when  $\alpha$  approaches the critical value (4.4), the Heisenberg orbits (as well as the Schrödinger wavepackets) start to expand beyond the limits permitted by (1.1), suggesting that the electrons confined in the standing wave (2.3) may produce some effects of anisotropic subcritical conductivity, nonpredictable on the basis of the 'effective potential' (1.1). Finally, if  $\alpha > \alpha_c$ , the polynomial (4.1) acquires two purely imaginary and four complex roots of the form  $\pm \zeta, \pm \zeta^*$  (where  $\text{Re } \zeta \neq 0$ ) causing an exponential explosion of all (but a subset of measure zero) of the canonical trajectories. Since this concerns the classical orbits passing arbitrarily close to the field center at  $\bar{x} = 0$ , we infer that the point  $\bar{x} = 0$  undergoes a structural metamorphosis, converting itself from an attractive into a repulsive center (Figure 1). As the same concerns all other nodal points (2.4), one is led to conclude that the standing wave trap (2.3) of sufficiently high intensity

$$B \cong \frac{2m\omega c}{e} \cdot \alpha_c \quad (4.5)$$

undergoes a qualitative change resembling the phase transitions. The weakest statement would be that when  $\alpha$  crosses  $\alpha_c$ , the approximation (1.1) based upon the potential  $V_{\text{eff}}$  with minima in the nodal points of (2.3), becomes qualitatively wrong. The centers of

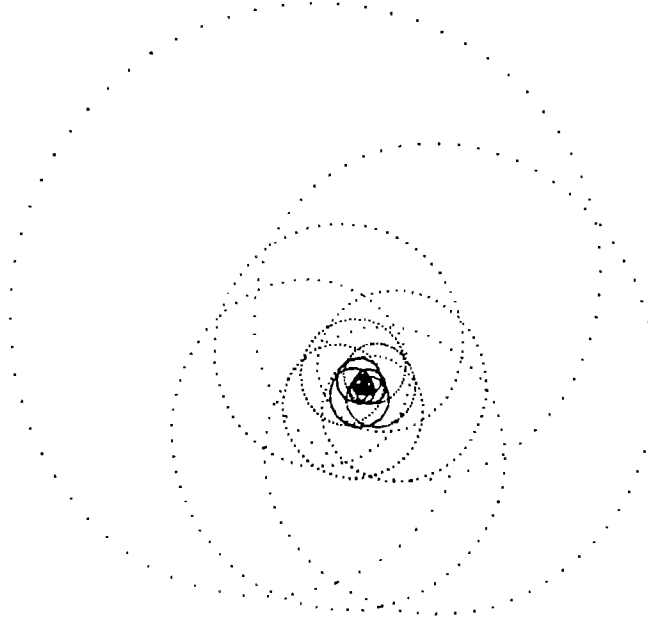


Fig. 1. The 'exponential explosion' at the nodal point of the field (2.3) for  $\alpha = 0.6$ ,  $\omega = 2\pi \times 10^{10}/\text{sec}$ . The computer was asked to determine numerically the motion of a classical test particle generated by 40 oscillations of the standing wave (2.3). The whole trajectory is contained in a narrow surrounding of the nodal point, of the diameter  $\delta = 10^{-5} \lambda$ , where the standing wave (2.3) can be substituted by (2.5) with a relative error  $< 10^{-10}$ . Were the effective potential (1.1) valid, the trajectory would not emerge from a sphere of radius  $\delta_0 = 4.4 \times 10^{-11} \text{ cm} = 1.45 \times 10^{-11} \lambda$  forming an invisible black dot in the center of our figure.

attraction previously existing in the points of  $\mathcal{N}$  are wiped out. The charged particle wandering around them can, perhaps, form some stable motion patterns but *not* of arbitrarily small size (this might correspond to a qualitative transition from the fix-points to the stable orbits in the abstract theory of dynamical systems [13]). A stronger hypothesis would be that the field (2.3), instead of serving as a particle trap, may acquire the properties of a particle repelling or particle transporting medium (though this still requires careful verification).

*Remark 1.* We have based our considerations on the specially simple structure of the field (2.3) in the vicinities of the nodal points (2.4). Besides  $\mathcal{N}$ , the standing wave (2.3) possesses two different classes of the nodal points where the behavior of the electromagnetic forces is no longer approximable by (2.5)–(2.6). It is to be presumed that the other critical values for  $\alpha$  may arise in relation to the field behavior around these centers. It is also to be expected that analogous stability thresholds might be associated with the nodal points of quite arbitrary standing waves.

*Remark 2.* The breaking of the 'high frequency approximation' which we have observed here is not an exception [which would occur only due to an intricate structure of the electromagnetic standing waves], but an example of a more general phenomenon which can be encountered in much simpler physical situations [14, 15].

### Acknowledgements

The authors are indebted to their colleagues in the Physics Department of the CINVESTAV, México, and in the Institute of Theoretical Physics of Warsaw University, Poland, for their comments and interest in this work. One of us (D.F.C.) is grateful for the kind hospitality at the Institute of Theoretical Physics of Warsaw University in November and December 1987. One of us (B.M.) would like to acknowledge the support of the interdisciplinary CPBP0103 grant.

### References

1. Phillips, W. D. and Metcalf, H. J., *Sci. Am.* **256** (3), 36 (1987).
2. Stenholm, S., *Rev. Mod. Phys.* **48**, 699 (1986).
3. Landau, L. D. and Lifshitz, E. M., *Mecanica*, Ed. Reverté S.A., Barcelona, México (1965).
4. Gaponov, A. V. and Miller, M. A., *JETP* **7**, 168 (1958).
5. Toschek, D. E., Atomic particles in traps, in G. Grynberg and R. Stora (eds.), *New Trends in Atomic Physics*, North-Holland, Amsterdam (1984);  
Brown, L. S. and Gabrielse, G.: *Rev. Mod. Phys.* **58**, 233 (1986).
6. Cook, R. J., Shankland, D. G., and Wells, A. L., *Phys. Rev.* **A31**, 564 (1985).
7. Hahn, E. L., *Phys. Rev.* **80**, 580 (1950).
8. Macomber, J. D., *The Dynamics of Spectroscopic Transitions*, Wiley, New York (1976).
9. Lewis, H. R. and Riesenfeld, W. B., *J. Math. Phys.* **10**, 1458 (1969).
10. Malkin, A., Man'ko, V. I., and Trifinow, D. A., *Phys. Rev.* **D2**, 1371 (1970).
11. Moshinsky, M. and Winsternitz, P., *J. Math. Phys.* **27**, 2290 (1986).
12. Mielnik, B. and Fernández, C. D. J., Electron trapped in rotating magnetic field, Preprint CINVESTAV, México, September 1987 (to appear in *J. Math. Phys.*).
13. Collet, P. and Eckmann, J. P., in A. Jaffe and D. Ruelle (eds.), *Iterated Maps on the Interval as Dynamical Systems*, Birkhäuser, Basle (1980).
14. Combesure, M., *Ann. Inst. Henri Poincaré* **44**, 293 (1986).
15. Mielnik, B., *J. Math. Phys.* **27**, 2290 (1986).